TGA and Time-Dependent FTIR Study of Dehydrating Nafion−Na Membrane

Yanqia Wang,[†] Yoshio Kawano,[‡] Steven R. Aubuchon,[§] and Richard A. Palmer*[,†]

Department of Chemistry, Duke University, Durham, North Carolina 27708-0346; Instituto de Química, Universidade de São Paulo, Caixa Postal 26077, CEP 05513-970, São Paulo-SP, Brazil; and TA Instruments-Waters, LLC., 109, Lukens Drive, New Castle, Delaware 19720

Received January 30, 2002

ABSTRACT: A detailed study of the dehydration process of hydrated Nafion−Na membranes has been performed using thermogravimetric analysis (TGA) and time-dependent (TD) FTIR, with the aim of investigating the water loss process during dehydration. The TGA data provide the absolute water weight loss, and TD FTIR spectra yield the relative IR intensity loss. Both TGA profiles and TD FTIR traces can be well fitted by second-order exponential decay, which implies two different dehydration processes, depending on water content. The fast process is attributable to high water level Nafion−Na (HWLN), with percolation structure and thus higher water diffusivity. The slow process is characteristic of low water level Nafion−Na (LWLN), with specific isolated cluster structure and lower diffusivity. For LWLN, the relative IR intensity loss of water bands is significantly faster and more extensive than the corresponding relative weight loss obtained by TGA. This deviation seriously calls into question the use of IR spectra as a quantitative measurement of water content in Nafion. The apparent dependence of the IR spectrum on the size of the nanoscale water clusters is in agreement with Gebel's mechanism of water swelling in Nafion.

Introduction

The use of perfluorosulfonated ionomers has substantially promoted the development of several important branches of the chemical industry, such as chlor-alkali technologies and methanol fuel cells. The structural details and properties of perfluorosulfonated ionomer membranes have been the objects of numerous theoretical and experimental efforts, as covered in Sondheimer's earlier review[1] and Heitner−Wirguin's more recent review.[2] The current understanding is based mainly on the results from studying Nafion **1**, the commercially available ionomer membrane film. The molecular structure of Nafion consists of a poly(tetrafluoroethylene) (PTFE) backbone with perfluorinated pendant chains terminated by sulfonate groups in either the acid (H^+) or neutralized (Na^+, K^+, etc.) forms.

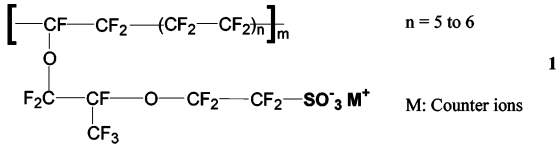

1

The structural nature of the ionomer leads to a phase separation, with the ionic groups aggregating into discrete domains separated by the low-dielectric polymer phase. It has been proposed and widely accepted that the microstructures of Nafion membrane can be understood in terms of a "reverse-micelle-like" cluster−network model.[3] As shown in Figure 1, the model assumes two fundamentally distinctive structural regions: the perfluorinated polymer network and the ionic clusters comprising sulfonate groups, countercations, and water molecules. In an ionic cluster, water molecules are found in the core, and sulfonate groups are found near the interface, extending into the water phase, and associated with the counterions. The neigh-

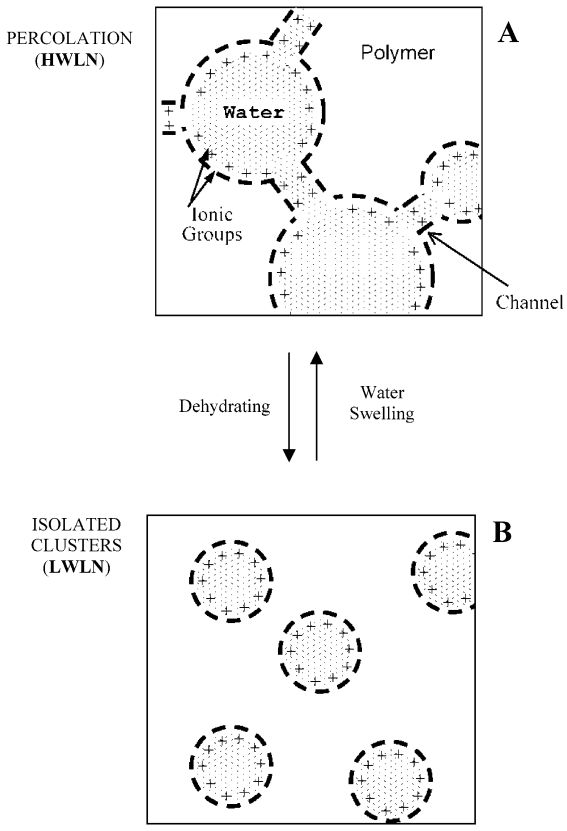

Figure 1. Schematic dynamic swelling and dehydration model for the low water level Nafion−Na. (+, −) mark ionic groups. (A) represents the percolation structure, with interconnected clusters, and (B) represents the structure, with isolated clusters. (A**)** and (B) have the same specific surface.[5]

[†] Duke University.
[‡] Universidade de São Paulo.
[§] TA Instruments-Waters, LLC.
* Corresponding author: e-mail rap@chem.duke.edu; phone (919)-660-1539; Fax (919)-660-1605.

10.1021/ma020156e CCC: $25.00
Published on Web 01/29/2003

boring clusters are presumably interconnected through channels that determine the transport properties of the ions and water. For instance, a percolation structure, which has well-connected cluster morphology, has higher ionic-exchange and water-diffusion rates than the isolated-cluster structure.[4] The supporting evidence for the percolation model for Nafion has come from small-angle X-ray scattering (SAXS) studies, which also have provided an estimate for a cluster diameter of ca. 4 nm and a channel diameter of ca. 1 nm (Figure 1).[5] Obviously, the cluster size and degree of interconnection are determined by water content and will change during the water swelling and dehydration processes.[6,7] For Nafion with very low water level, the intercluster channels may disappear, and the clusters tend to be isolated from each other. A quite clear description of the swelling process has been represented by Gebel [5] and by others.[8,10,11] A swelling mechanism is proposed, involving a structural reorganization, which is characterized by a cluster number decrease and an intercluster distance increase (Figure 1). A conversion from isolated cluster to percolation structure occurs in the swelling process and from percolation to isolated cluster structure in the dehydration process. The extent of cluster structure has a marked influence on the physical properties of Nafion, such as its ionic exchange ability and rheological responses.[2,12]

Many techniques have been used to investigate the water component in Nafion membranes.[4,7,10,13−16] Among these, thermogravimetric analysis (TGA) is one that can accurately determine the absolute water content of Nafion−Na and dynamically monitor the water loss as a function of time and temperature. For Nafion, the dehydration process can be easily distinguished from thermal decomposition, due to Nafion's high thermal stability. Furthermore, the weight loss and water loss can be quantitatively correlated over a wide range below the thermal decomposition temperature.[8−11] FTIR spectroscopy has also been used as another powerful tool to study the water component in Nafion.[13] Very detailed information has been obtained by analyzing the HOH bending and OH stretching mode regions. The OH stretching mode, giving rise to a broad and prominent absorption between 4000 and 3000 cm^{-1}, provides important corroboration of the structure in the nanoscale water clusters. The HOH bending fundamental mode, peaking at ∼1628 cm^{-1}, has been used as a quantitative measure of water content by either its integrated absorbance or peak absorbance.[1,17−21]

However, some recent studies suggest that quantitative water content measurement by IR may not be reliable in Nafion, especially for very low water levels.[22−24] The key presumption of quantitative water determination with IR spectra is Beer's law, in which the absorbance intensity is linearly dependent on concentration. However, for D_2O clusters in aerosols within the 2−12 nm diameter range, Devlin and co-workers have found that Beer's law may not be applicable. For these nanoscale water clusters in aerosols, the IR spectrum of water not only is dependent on the total water content of the aerosol but also apparently depends on the size of the clusters.[22,23] In Nafion the imbedded water clusters are also in this nanoscale range, and therefore, it is reasonable to expect a difference between the true water concentration change and the water IR spectrum change in Nafion during the hydration and dehydration processes.

In the present work, we compare the weight loss profiles obtained by TGA and parallel water IR absorption intensity loss traces obtained by FTIR. Nafion−Na is used in our experiment owing to its higher stability relative to the acid form, less obscured IR spectra, and as a representative of other alkali-loaded Nafions. The TGA weight loss profiles can be quantitatively associated with the loss of the water. However, the more rapidly changing OH stretching and HOH bending IR absorption bands strongly support the proposition of the dependence of the IR on the size of the nanoscale water clusters. Analysis of the results is shown to be consistent with Gebel's swelling mechanism for Nafion as well as Devlin's observation on D_2O aerosols. This work is significant for deeper understanding of the structural evolution of Nafion clusters during dehydration, as well as for understanding other processes involving cluster development such as changes in mechanical properties.

Experimental Section

Sample Preparation. Nafion-117 membrane with an equivalent mass of 1100 and thickness of 0.175 mm was provided by E.I. Du Pont de Nemours & Co. The membrane samples were purified to remove colored impurities by means of the usual procedure.[4] In the purification, the membranes were first submerged in concentrated nitric acid with stirring at 60 °C for 24 h. The acid was then decanted, and the films were placed sequentially in 60, 40, and 20% nitric acid, each for 1 h, with stirring, followed by washing thoroughly with deionized water. The treated acid form films are colorless and transparent to the eye. Conversion of the membrane samples to the sodium form was achieved by soaking the treated films in 1 M aqueous sodium chloride with stirring for 24 h, immediately followed (see below) by parallel TGA and FTIR measurements. The Nafion−Na is also colorless and transparent to the eye, with 0.175 mm thickness. The specimens for TGA measurements were prepared by cutting the hydrated membranes into strips weighing about 5−10 mg to fit the TGA crucible. The specimens for time-domain FTIR experiments were cut from the same membrane as the TGA samples, but with a rectangular shape of 7 × 20 mm. The specimens for photoacoustic spectroscopy (PAS) were cut to square strips of 5 × 5 mm.

Time-Dependent and Temperature-Dependent Thermogravimetric Analysis. The sample was taken from the salt bath, rinsed thoroughly with deionized water, blotted dry, and placed immediately in the TGA platinum sample pan (ca. 1 min elapsed time). An additional 1.2 min of mass and temperature equilibration then elapsed before data recording commenced. TGA measurements were carried out in two successive steps with the same specimen, on a computer-controlled TGA model Q500 (TA Instruments-Waters, LLC., New Castle, DE). In the first step, the isothermal weight loss was recorded over 24 h. The sample was kept at a constant 25 °C under a dry nitrogen atmosphere (40 mL/min). In the following step, the same specimen was heated from ambient to 500 °C at a rate of 20 °C/min. The Hi-Res TGA mode was used to optimize weight loss resolution of 0.3 °C.

Time-Dependent (Isothermal) FTIR Measurement. The sample was rinsed and blotted dry as for the TGA measurements. TD FTIR spectra were collected on a Bruker Optics IFS66/s spectrometer equipped with a DTGS detector. No optical or electronic filters were used. The membrane was self-supported on the sample holder under a dry CO_2-free air atmosphere, and after a 1 min delay to match the TGA equilibration time, the absorption spectra were measured by the transmission method, in the continuous-scan time-resolved mode. A total of 128 scans were averaged per spectrum, and 30 spectra were recorded per hour. Each spectrum was recorded from 7000 to 400 cm^{-1} at 25 °C, with a spectral resolution of 4 cm^{-1}, a phase correlation of 8 cm^{-1}, and an

Table 1. Second-Order Exponential Fitting Results of the Isothermal Water Loss Profile and Relative IR Intensity Traces for Dehydrating Nafion−Na

	fitting function: $Y = Y_0 + A_1e^{-t/t_1} + A_2e^{-t/t_2}$			
fitting results	TGA weigh loss	CF_2 combination[a]	water stretching	water bending
χ^2 (chi square value of fit)	3.92×10^{-5}	3.47×10^{-6}	3.58×10^{-5}	3.42×10^{-5}
R^2 (coefficient of determination)	0.983	0.990	0.996	0.996
t_1 (min)	6.3 ± 0.1	7.9 ± 0.2	17.4 ± 0.4	20.6 ± 0.4
t_2 (min)	288 ± 2	246 ± 4	500 ± 6	502 ± 7

[a] The reciprocal of the intensity is used for decay fitting.

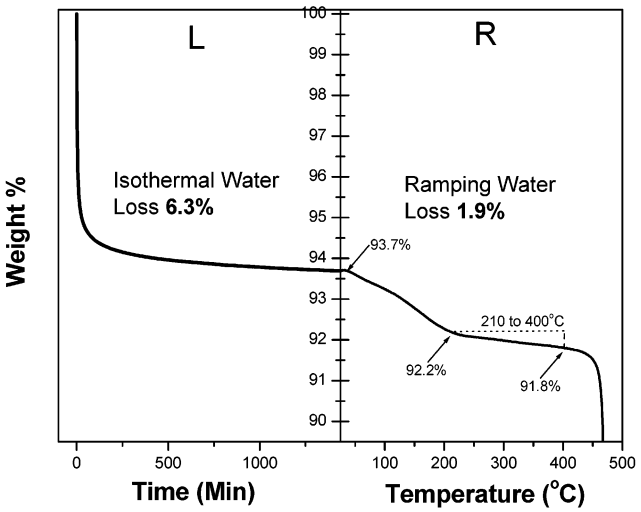

Figure 2. TGA weight loss profiles of Nafion−Na dehydration: (L**)** isothermal weight loss of fully hydrated membranes for 1500 min under negligible humidity; (R**)** temperature-domain weight loss of the membrane after the L measurement.

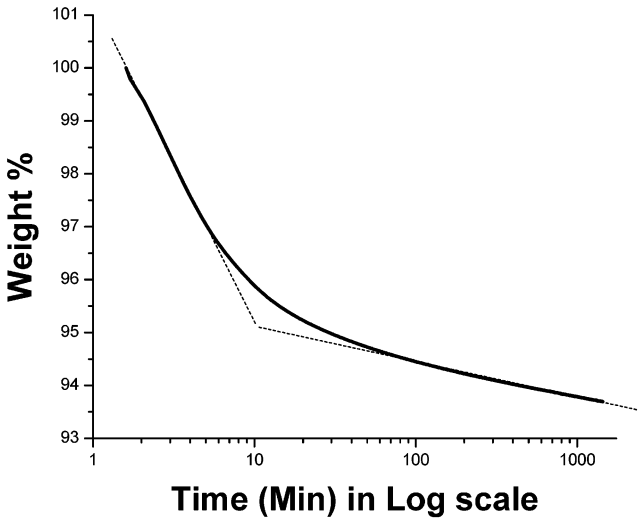

Figure 3. Isothermal weight loss of fully hydrated Nafion−Na membranes for 1500 min under negligible humidity in log scale to show dual-dehydration stages.

aperture setting of 2 mm. All spectra were compared to the same open-beam background spectrum. The experiment was repeated for 10 times with no significant difference in band intensities or shapes. The shown one is the one with best quality whose values are very close to the average of all trails.

Photoacoustic Measurement. PAS experiments were performed by use of a MTEC model 300 photoacoustic cell, with helium as transfer gas, on the Bruker Optics IFS66/s spectrometer. No optical or electronic filters were used. The spectra were obtained using the continuous-scan mode, and a total of 64 scans were averaged. The spectra were recorded from 4000 to 400 cm^{-1} at 25 °C, with a resolution of 4 cm^{-1} and an aperture setting of 8 mm. The PA measurements were repeated over 10 times.

The TGA measurements and data were controlled and processed using Thermal Advantage and Universal Analysis 2000 software in the WinNT 4.0 operation system. The FTIR data were collected and analyzed by software from Bruker Optics Inc., OPUS version 3.0 in the OS2 operating system. The curve fitting and graphing were accomplished with Microcal Origin, version 6.0.

Results

The TGA weight loss profiles are shown in Figure 2. Figure 2L represents the isothermal weight loss profile of fully hydrated Nafion−Na at 25 °C, and Figure 2R is the subsequently measured temperature-dependent weight loss profile of the same sample. The log of the isothermal weight loss profile (Figure 3) indicates clearly the dual-stage dehydration process. The isothermal water loss data were fitted with a second-order exponential expression, and the fitting results are shown in Table 1. The fitting results of the relative IR integrated intensity change traces are also shown in Table 1.

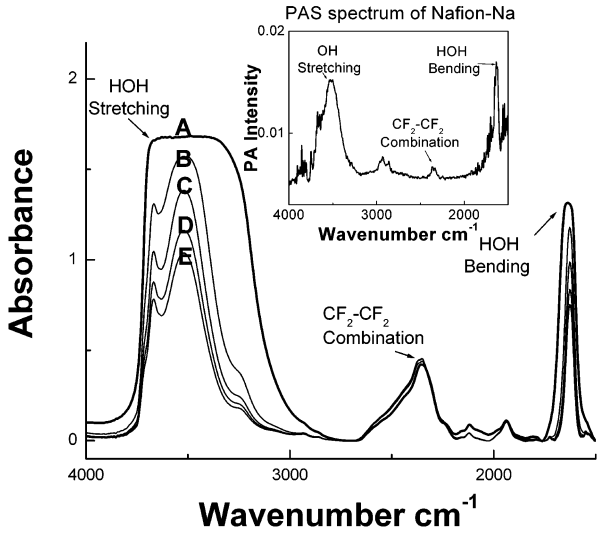

Figure 4. Infrared spectra of Nafion−Na (4000−1500 cm^{-1}) at different dehydration times: (A) fully hydrated, $t = 0$; (B) $t = 100$ min; (C) $t = 495$ min; (D) $t = 950$ min; (E) $t = 1450$ min.

Selected FTIR spectra of dehydrating Nafion−Na at different times are shown in Figure 4 in order to provide a direct view of the tendency of the intensity changes. A PA spectrum of Nafion−Na is presented as an inset. The wavenumbers and assignments of the OH stretching fundamental, HOH bending fundamental, and CF_2 stretching combination band are listed in Table 2. Table 3 records the dimensional change of a Nafion−Na membrane specimen, from before to after dehydration. Figure 5 shows the OH stretching fundamental mode of LWLN and its curve fitting calculation from 4000 to

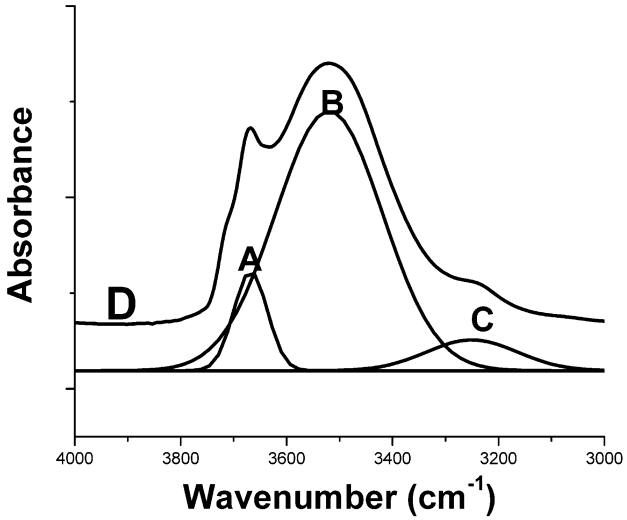

Figure 5. OH stretching region of LWLN: (**A**) subband at ∼3680 cm^{-1}, cluster surface water; (**B**) subband at ∼3520 cm^{-1}, cluster core water; (**C**) shoulder at ∼3250 cm^{-1}, OH bending overtone; (**D**) total band from 4000 to 3000 cm^{-1}. **D** is shifted upward for a clear view.

Table 2. Selected Infrared Absorption Bands of Nafion−Na

band position (cm^{-1})	assignments	integrated intensity (area)
1628	HOH bending fundamental	1730 to 1590 cm^{-1}
∼2360	CF_2 stretching combination ($1152_{(sym)} + 1213_{(asym)}$)	2700 to 2200 cm^{-1}
∼3250	HOH bending overtone (∼ 2 × 1628)	over all band is integrated from 3750 to 3000 cm^{-1}
∼3500 to ∼3520	OH stretching fundamental O—H····O, cluster core water	
∼3670	OH stretching fundamental O−H· · ·CF_2, cluster surface water	subbands achieved through peak-fitting

Table 3. Shrinkage of Nafion−Na Membrane on Dehydrating

	thickness (mm)	width (mm)	length (mm)
fully hydrated	0.175 ± 0.003	6.8 ± 0.1	21.9 ± 0.1
dry	0.175 ± 0.003	6.2 ± 0.1	20.0 ± 0.1
shrinkage (%)	∼0	∼10	∼10

3000 cm^{-1}. Two subbands are labeled **A** and **B**, the shoulder is labeled **C**, and the original spectrum is labeled as **D**. **D** is shifted upward for a clear view. The normalized relative intensity of the IR bands, subbands, and shoulder in the water stretching region after 100 min of the isothermal experiment are presented in Figure 6 to show the different decreasing rates of the cluster surface water and the cluster core water. The curves are identically labeled as in Figure 5.

The time-dependent relative integrated IR band intensity traces of the OH stretching mode, HOH bending mode, and CF_2 combination band are normalized to their starting intensities and shown in Figure 7. The traces were all fitted with second-order exponentials, and the results are shown in Table 1. (The reciprocal of the intensity of the CF_2 combination band is used to make the fitting possible.) Figure 8 shows the comparison of the renormalized relative IR traces of the

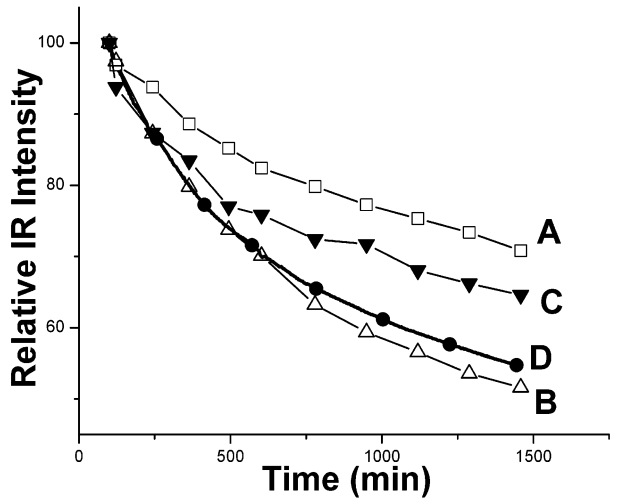

Figure 6. Relative IR intensity loss traces of the OH stretching mode and its decompositions: (**A**) subband (□), cluster surface water; (**B**) subband at ∼3520 cm^{-1} (△), cluster core water; (**C**) shoulder at ∼3250 cm^{-1} (▼), OH bending overtone; (**D**) total band from 4000 to 3000 cm^{-1} (●).

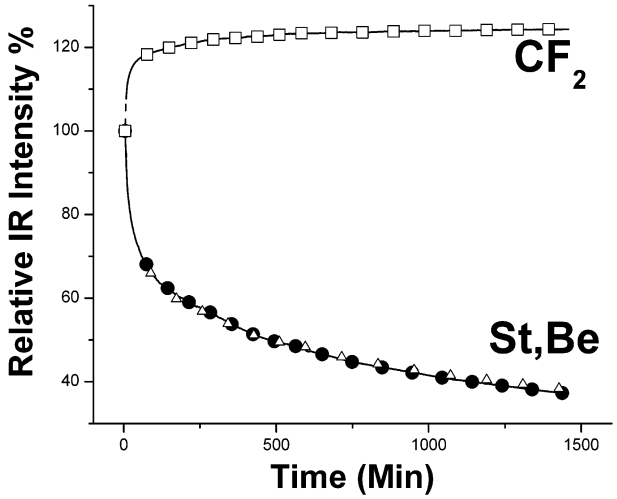

Figure 7. Normalized relative IR band intensity and weight loss traces from 100 to 1500 min: (**St**) OH stretching mode (●), (**Be**) HOH bending mode (△), (**CF_2**) CF_2 combination **C** (□). Initial values are defined as 100%.

OH stretching mode, labeled **St**, HOH bending mode, labeled **Be**, and weight loss, labeled **Wei**.

Only the data points after 100 min are selected to represent the LWLN to eliminate the influence of IR saturation at the beginning of the measurement. The values of the water percentage and the IR intensity at 100 min are set as 100% for renormalization. Additionally, the IR traces are further renormalized with the CF_2 combination trace to eliminate the dimensional change influence.

Discussion

From the TGA data, the weight loss is analyzed to obtain the absolute water content (Figure 2). Since, based on the structure and thermal stability studies of Nafion−Na, water is the only volatile component at room conditions (25 °C, 1 atm), the isothermal weight loss (Figure 2L) can be completely attributed to the water loss. An initial amount of water (6.3% of total weight; 100.0%−93.7%) is lost after 1500 min. However, this amount is smaller than the total water content,

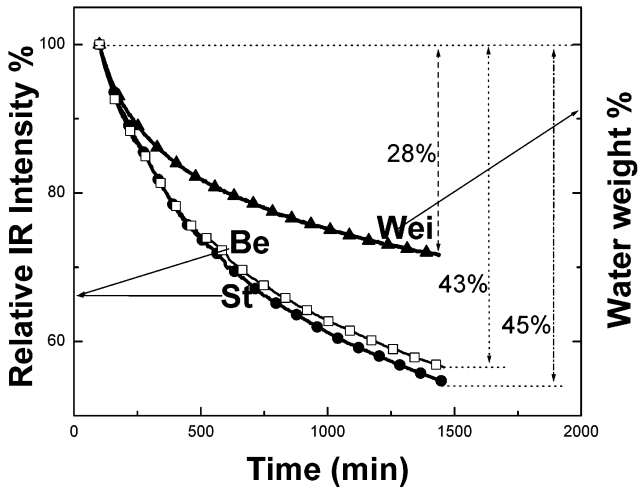

Figure 8. Renormalized relative IR band intensity traces and weight loss profile after 100 min: (**St**) OH stretching mode (●), (**Be**) HOH bending mode (□), (**Wei**) weight loss profile (▲). Values at 100 min are defined as 100%. Trace **St** and **Be** are also normalized to the CF_2 combination IR trace to eliminate shrinkage influence.

because it is impossible to obtain a fully anhydrous Nafion at room temperature despite the negligible humidity environment in the TGA sample crucible.[18,25] The highly dipolar ionic groups firmly retain a certain amount of water. To determine the total content, the temperature-dependent TGA measurement is indispensable.

Two distinct decay processes are suggested in the observed isothermal weight loss profile (Figure 3), which are attributed to the loss of "bonding water" (water molecules embedded in the structure, bonding with each other, and/or with the ionic moieties). Clearly, before the bonding water loss, a even faster dehydration corresponding to loss of water on the surface of the membranes is expected, which would then indicate a *three*-stage isothermal decay curve. However, in the experiment, the surface water loss is not be detected due to the limitation of the instrument and the experimental procedure. As described in the Experimental Section, sample handling and instrument equilibration introduce a "dead time" of approximately 2 min. It is reasonable to assume that virtually all the surface water is lost during this dead time. Supportive evidence comes from the curve-fitting results in Table 1. The fast TGA isothermal water loss process has a decay time of about 6 min, while the surface water loss is believed to be much faster than that. If we propose a one-tenth decay time relationship (0.6 min), it is safe to say that most of the surface water loss process has been finished before the measurement starts.

The weight loss profile is fitted with second-order exponential (expression shown in Table 1), which yields good fitting results (Table 1). The third-order exponential decay is not significantly better than the second-order exponential decay fitting (e.g., the R^2 for third and second fitting of TGA isothermal profile are 0.990 and 0.983, respectively). The large difference between the two decay times, 6.3 and 288 min, is correlated with two distinct dehydration mechanisms. The fast dehydration process occurs at the beginning of the measurement and corresponds to HWLN, whereas the slow dehydration process is correlated with LWLN. The transition is assumed to be associated with the different cluster morphologies in HWLN and LWLN.[5,7]

The morphology of clusters in Nafion−Na is strongly determined by water content. The cluster shape in Nafion is believed to be determined by the electroelastic interaction energy between the ionic clusters and the fluorocarbon matrix and the surface energy of the cluster.[6,7] For LWLN, both theoretical micromechanical approaches and experimental SAXS results support the model of roughly spherical isolated clusters. For HWLN, spherical shape is still believed to be the best approximation for the percolation structure (see above, Figure 1).[16,26] Even though the exact size average and the size distribution of Nafion clusters are difficult to measure, it is almost certain that the clusters are within the nanoscale range (1−10 nm). For instance, the estimate made by Gebel suggests that the cluster diameters in dry, slightly swollen, and percolation Nafion are about 1.5, 2.0, and 4.0 nm, respectively.[5] However, a quantitative relationship between the cluster size and water content in Nafion has not yet been successfully derived.

On the basis of small-angle neutron scattering (SANS) studies, the schematic evolution of the clusters during the swelling process is as represented in Figure 1.[5] Figure 1A represents the percolation structure of more-swollen Nafion, which can be qualitatively associated with HWLN in our study. Figure 1B represents the structure of less-swollen Nafion characterized by the presence of isolated spherical clusters, which can be similarly associated with LWLN. For a better description of the structure evolution in Nafion, the specific surface (SS), the area of the polymer−water interface per polar head, is used because the small-angle scattering data indicate that SS is independent of the water content.[7,27] In Gebel's mechanism, during water swelling (B to A), the first consequence is the volume increase of individual clusters. After that, further coalescing of clusters occurs in order to maintain a constant SS and the equilibrium density of ionic groups on the surfaces of the aggregates. This fusion results in a decrease of the total cluster number and an increase of the intercluster distance. The net outcome is that the rate of increase in average cluster volume is faster than the rate of the increase of water concentration. An opposite structural reconstruction is expected to occur in the dehydration process, that is, cluster splitting increases the total cluster number, which causes a faster and greater average cluster size decrease than predicted for a constant cluster number.

The water diffusivities (WD) of different cluster structures of Nafion are predictably different. Percolation Nafion has higher WD than isolated-cluster Nafion, because in the former case, water molecules can be transported to the surface of the membrane relatively easily through the intercluster channels. The transition between percolation and isolated cluster structure suggests a water level threshold around which the conversion occurs. The percolation threshold hypothesis is experimentally supported by the work of Freger and coworkers, who measured the WD coefficients in some ionic and nonionic polymers by the pulsed-gradient spin-echo NMR method.[15,28] Their results show that the WD in Nafion is remarkably different from that in other ion-exchange membranes. WD in Nafion does not exhibit a consistent dependence on the volume fraction of the water over the whole concentration range.[15,28] In isothermal dehydration, as the water content decreases with time, the percolation structure is converted into

the isolated cluster structure, together with an increasing length or even closure of the intercluster channels. This structural conversion greatly lowers the water diffusivity and obstructs the water loss process.

The temperature-domain TGA behavior of Nafion−Na (Figure 3B) is quite consistent with that reported for neutralized Nafion.[8,9,11] Additional weight loss is observed in two different stages occurring before the thermal decomposition occurs at about 460 °C. The first stage, from 26 to 210 °C, is far below the thermal decomposition temperature, and weight loss in this regime is still approximately consistent with water loss. However, total removal of water is not yet complete in this stage. According to the literature,[17] it is difficult to obtain a fully anhydrous Nafion membrane without destroying the membrane. Removing all the water molecules requires ca. 250 °C and an equilibration time of hours. Needless to say, for the temperature-domain TGA measurement with the ramping rate of 20 °C/min, even higher temperature is needed to reach the totally anhydrous condition.

In the subsequent, more gradually decreasing loss process, from 210 to 400 °C loss process, the association between weight loss and water loss is less certain. In this range, other sources such as impurities and additives might contribute to the weight loss as well. However, the weight loss is probably still mainly determined by the loss of residual water molecules that are directly coordinated with the ionic groups. Thus, below 400 °C, the total weight loss can be approximated as the water loss without significant errors because the weight loss (0.4%) in this last stage (210−400 °C) is a small fraction of the total weight loss (∼8%), and in any event, only the "relative" water loss is used in our discussion. The water loss at 400 °C is selected as the total water content of the fully hydrated Nafion−Na membrane measured. Its value, 8.2%, equals the summation of the isothermal loss of 6.3% and the additional temperature-dependent loss of 1.9%.

Parallel to the TGA measurements, IR spectra were also collected for the isothermal dehydration process of fully hydrated Nafion−Na membranes. Whereas in the TGA measurement, the weight loss is exclusively and linearly dependent on the water content, the analysis of the IR spectra is more problematic. However, the interpretation of the IR spectra of water clusters in other environments offers helpful clues to understand the Nafion data. In molecular beam experiments, the IR spectra of small water clusters $(H_2O)_n$ ($n < 10$) have been shown to vary noticeably even with small changes of n.[29,30] Other recent attempts have been made to investigate IR spectra of nanoscale water clusters containing hundreds to thousands of water molecules.[22,23] These studies on the IR spectra of aerosols of D_2O clusters with average diameters in the 2−12 nm range showed that the area of the O−D stretching mode absorption band is proportional to the average cluster size.[22,23] According to the authors, in this size range, unlike in bulk water, clusters can be viewed as composed of a central crystalline core, a disordered surface, and a strained subsurface region that joins the core and surface. The surface and subsurface water molecules of the clusters occupy a quite high volume fraction for nanoscale clusters. The size dependence effect has been ascribed to the diminution of the fraction of crystalline core molecules with decreasing cluster size. Thus, it is reasonable to attempt to explain the Nafion water IR spectra as reflecting a combination of dependence on water content and cluster size.

Because of the thickness of the Nafion-117 membrane (∼0.175 mm), most of the mid-IR absorption bands, especially those below 1500 cm^{-1}, are completely saturated in the transmission mode measurement and thus provide no useful information. Surface IR techniques, such as attenuated total reflectance (ATR) or photoacoustic spectroscopy (PAS), cannot be used to determine the overall water component because of the possible inhomogeneous water distribution in such thick membranes. Fortunately, not all the absorption bands are totally saturated (Figure 4). The HOH bending fundamental mode (ν_2) and OH stretching fundamental mode (ν_1) are saturated during the early part of the dehydration due to high water content but are unsaturated at later times. The CF_2 stretching combination mode is unsaturated throughout the measurement. All these bands have prominent absorbance and are free of the interference from the other major Nafion absorptions, which makes them suitable for quantitative analysis. The OH vibrational modes provide information on the structure and concentration evolution of the water component, and the CF_2 combination band provides information on the dimensional changes of the polymer network.

All Nafion membranes exhibit prominent water bands except for extremely dried specimens. Unlike the single broad OH stretching fundamental band of liquid water from 4000 to 3000 cm^{-1} (ν_1), the spectrum of LWLN is much more complicated. This region provides information concerning hydrogen bonding of water and thus reflects the environment of the water molecules. The Nafion−Na spectrum in this region can be approximately decomposed into two subbands and a shoulder (Figure 5).[17−21] The two distinguishing subbands, at 3670 and 3520 cm^{-1}, labeled **A** and **B**, are assigned to the OH stretching fundamental modes of water in two distinct environments. The weak subband **A** is believed to be representative of water molecules on the periphery, or surface, of the clusters, with one or both OH groups exposed to the fluorocarbon environment. The frequency of subband **A** is close enough to that of the gas-phase OH stretching mode that it must be considered due to the OH groups **not** involved in O−H···O hydrogen bonding. These water molecules, located in the interfacial region between the clusters and the polymer matrix or in the channels between clusters, are less ordered, and thus are termed "free water" by some researchers.[18] At the same time, the strong main subband **B** is associated with those water molecules in the core of the aqueous medium, whose hydrogen bonding is in forms such as water···water and water···sulfonate. Subband **B** thus belongs to water molecules with restricted mobility, which are termed "freezing water".[18] For a better description, in this report, we will use "cluster surface water (CSW)" for "free water" and "cluster core water (CCW)" for "freezing water". In LWLN, the sum of the CSW and CCW comprises virtually all of the "bonding water". The ratio of **A** and **B** band intensity is found to be inversely proportional to cluster size.[22,23] The shoulder **C**, at about 3250 cm^{-1}, is assigned to the overtone of the HOH bending mode ($2\nu_2$). The relative intensity trace of this band (Figure 6) is presented but not discussed in detail because it shows much broader and more variable bandwidth in the curve-fitting process; additionally, its intensity is weaker than **A** and **B** subbands.

Since subband **B** has the largest fraction of the total intensity, trace **B** is close to the total intensity loss, trace **D** (Figure 6). At the same time, trace **A** exhibits a distinctly slower decreasing rate than trace **D**. This indicates that the ratio between CSW (**A**) and CCW (**B)** increases during the dehydration process, which is consistent with the prediction of the decreasing cluster size and the (relatively faster) removal of CCW. The IR spectra and peak fitting distinctly show that there are two populations of water in the clusters, CSW and CCW, which suggests a dual-dehydration process in LWLN. However, the expected dual dehydration is not observed in the TGA isothermal weight loss profile, whose curve-fitting results suggest a fast and a slow process corresponding to HWLN and LWLN, respectively, that is, a single dehydration in LWLN. Two possible mechanisms can be proposed. In the first one, CSW and CCW are lost independently and simultaneously, each with its own rate. For this mechanism, the reason we do not observe two independent processes would be due to the loss rates of CSW and CCW being very close to each other. Another mechanism is that CSW and CCW are in a relatively rapid dynamic equilibrium, and only one of the two species is lost. If this is the mechanism, we would again observe a single dehydration rate in LWLN. At this point, it is not possible to distinguish between these two possibilities.

In the near-IR (NIR) region, near 5350 cm^{-1}, a very broad band assigned to the combination of HOH stretching and bending modes can be observed (not shown in figures), which is not saturated throughout the dehydration. However, the intensity of this band is so weak that it is unsuitable for quantitative analysis.

It is the HOH bending fundamental mode (ν_2), peaking at ~1628 cm^{-1}, that is frequently utilized as the quantitative measurement of water content through its integrated absorbance or peak absorbance. Some supportive evidence and examples were presented in Falk's report.[13] The use of this band is feasible because it is totally clear of interferences from other major Nafion absorptions. The use of the bending mode intensity has been thought to be a considerable improvement over weighing techniques for determining the actual water content in the Nafion membrane.[13]

The CF_2 combination mode at 2360 cm^{-1} can also provide important information about thick Nafion membranes. This absorption has been underestimated or even ignored previously, apparently, because of its near coincidence with the gas-phase CO_2 stretching mode and its weakness in the attenuated total reflectance (ATR) and PA spectra which are routinely used for IR measurements on thick Nafion (see, for example, inset in Figure 4). In the transmission mode, the absorbance of the CF_2 combination band is greatly intensified, which makes it suitable for quantitative use. In our research, this absorption has been used to monitor the dimensional development of the Nafion network during dehydration.

Without noticeable wavenumber shifts, the intensity changes of the three bands (3670, 3520, and 2360 cm^{-1}) during dehydration can be classified into two distinctive tendencies: the decreasing water absorptions and the increasing backbone absorption (Figure 7). The traces of the water band intensities are clearly associated with the removal of water during dehydration. At the same time, the trace of the CF_2 combination band absorption can be interpreted as indicating shrinkage during dehydration. Even though dehydration causes a decreasing water fraction and a complementary increasing polymer fraction, the intensity of the backbone CF_2 absorption is presumed to be constant if the volume stays constant, since the moles of polymer contributing to the IR absorption do not change with constant sample volume. However, an anisotropic shrinkage is confirmed by the dimensional measurement of the Nafion−Na membranes (Table 3). The width and length of the sample in the dry state are about 10% less than those in the water-saturated state, but the thickness is constant. The dimensional change is quite consistent with the relative intensity gain trace of the CF_2 combination band, whose final intensity is about 24% larger than the initial value.

The relative IR intensity traces of the water and backbone absorptions, as well as the isothermal weight loss trace, can be well fitted with second-order exponentials (Table 1). All traces indicate two dehydration processes, with different rates. Since the backbone absorption is unsaturated throughout the measurement, not surprisingly, it gives decay times (7.9 min/246 min) which are consistent with those of the weight loss trace (6.3 min/288 min). However, significant deviations are observed for the water IR absorption loss traces, whose dual decay times are 17.4 min/500 min (stretching) and 20.6 min/502 min (bending). Thus, the water band traces show a distinctly slower rate of decrease than the weight loss and CF_2 combination band traces, both early and late in the dehydration process.

In the first phase, the superficial inconsistency between the fast weight loss and the slower change in water IR bands (6.3 vs 20 min) can be partially attributed to partial saturation of both the water stretching and bending fundamental absorption bands in the early part of the process. During the beginning stage, the water content is high, and the recorded water absorption is lower than the actual intensity due to the saturation. However, the same interpretation does not apply to the later times. To make a more reliable comparison of the actual water loss and IR intensity loss, only the spectra at later time (>100 min) are used. These spectra are associated with LWLN and the isolated cluster structure.

As discussed before, the relative weight change is strictly proportional to the relative water concentration change

$$RW_t = W_t/W_I = c_t/c_I \tag{1}$$

where RW_t stands for the relative water weight at time t, W_t stands for the absolute water weight at time t, W_I stands for the initial (t = 100 min) water weight, c_t stands for the water concentration at time t, and c_I stands for the initial (t = 100 min) water concentration.

Ideally, if Beer's law is also strictly followed, which means that the IR water band intensity is solely determined by the water concentration, we have a similar expression as for IR intensity

$$RA_{ct} = A_t/A_I = c_t/c_I \tag{2}$$

where RA_{ct} is the relative water IR intensity at time t when only concentration is considered, A_t is the actual water IR absorbance intensity at time t, and W_I is the initial (t = 100 min) water IR absorbance intensity. Under these ideal conditions, a proportional relationship between the weight loss and the IR inten-

Table 4. Estimate ΔRA_{e1500} for HOH Bending Intensity

	RW_{1500} or RA_{c1500} (%)	F_{s1500}	ΔRA_{e1500} (%)	actual loss (%)	note
a	72	1	28 ± 4	45	concn influence
b	72	0.9	35 ± 5	45	add size influence
c	72	<0.9	>35	45	add cluster splitting

sity loss is expected as eq 3

$$RW_t = RA_{ct} \tag{3}$$

For a clarity, several variables are defined in expressions 4−6

$$\Delta RA_{et} = 100\% - RA_{ct} \times F_{st} \tag{4}$$

$$F_{st} = Cd_t/Cd_I \tag{5}$$

$F_{st} = 1$
if only concentration influence is considered (6)

where ΔRA_{et} is the "expected" relative absorbance decrement with ±15% error range at time t,[13] F_{st} is the cluster size influence at time t, Cd_t is the relative average diameter of water clusters at time t, and Cd_I is the initial (t = 100 min) average diameter of water clusters.

The isothermal water weight loss curve and IR intensity loss curves of LWLN at later times (> 100 min) are compared in Figure 8, and the calculated results for time 1500 min are listed in Table 4. For this particular time, the weight loss curve (labeled as C) shows a relative decrement of 28% (100% − RW_{1500}, where RW_{1500} = 72%). If only the concentration influence is considered (RA_{c1500} = 72% and F_{s1500} = 1), the corresponding ΔRA_{e1500} should also be 28 ± 4%. However, the actual relative decrements of IR intensities, 45% (HOH bending, labeled **Be**) and 43% (HOH stretching, labeled **St**), are clearly beyond this range. The significant deviations strongly indicate that concentration itself is not adequate to explain the actual IR intensity change. In the following discussion, only the bending band trace will be discussed in detail because the bending and stretching intensity traces are quantitatively very close, and similar results are acquired through an identical analysis process.

The inconsistency is interpretable by introducing the IR size dependence and the swelling mechanism discussed above. On the basis of the morphology model, within a certain volume of the material, it is reasonable to assume an approximate proportional relationship between the total volume of the water clusters and the total number of the water molecules (or the water concentration). On the basis of this assumption and eq 1, it is possible for us to estimate the relative dimensional changes through the relative weight loss.

If the total number of clusters remains constant, the relative average water cluster diameter (assuming spherical clusters) can be calculated through the volume/diameter relationship. Thus, F_{s1500} should be 0.90 ($(0.72)^{1/3}$). So, if the IR intensity is directly proportional to cluster size, this would predict that ΔRA_{e1500} should be ca. 35% (100% − 72% × 0.9), still somewhat below the observed 45%. However, consideration of Gabel's mechanism actually predicts that the cluster size will be smaller than predicted by the loss of water volume alone. This is due to the cluster splitting process required to maintain the SS as the volume decreases. Therefore, F_{s1500} is expected to be smaller than 0.90, and the predicted ΔRA_{e1500} would continue to approach the observed absorbance loss. Unfortunately, an exact calculation cannot be made in the absence of a quantitative model for the cluster splitting process.

From the data presented here, it must be concluded that reliance on the change in IR intensity of water-related bands to judge the water content of Nafion is not warranted. However, despite the semiquantitative consistency of the analysis presented, it must be admitted that this does not constitute proof of the cause and effect relationship of cluster size and IR intensity. Even though Gebel's mechanism is based on experimental results, the exact mechanism is not completely certain.[5] Second, the cluster size-dependent IR spectra in the literature were obtained under quite different conditions. In Devlin's work, D_2O aerosols were prepared and measured under vacuum at 100 K. However, in the work reported here, the water clusters are embedded in a hydrophobic environment, and the spectra are measured at 298 K under 1 atm.[22,23] Additionally, Nafion water clusters are solution-like because ionic groups are included, whereas Devlin's water clusters were in pure form.[22,23] Finally, the actual quantitative correlation between water spectra and water cluster size is not well-defined. The proportional size dependence based on Delvin's observation requires more supportive experimental evidence. We are indebted to a referee for the suggestion that free energy differences between the different types of water in the clusters may offer an alternative explanation. Such a model is the object of ongoing theoretical effort. However, regardless of the ultimately most successful model, the significant deviation of the water IR band intensity change from the change in water content of Nafion membrane is experimental fact.

Summary

This is the first report investigating possible cluster size-dependent water IR spectra in hydrated Nafion−Na. TGA measurement reveals the water content and monitors the dynamic weight loss in the dehydration process. For temperatures far below the thermal decomposition of the material, the weight loss can be quantitatively correlated with water content. The TGA measurement shows that Nafion−Na membranes retain a small amount of water even under negligible humidity environment at ambient conditions. Removal of all water is accomplished at about 400 °C. The isothermal water loss can be decomposed into two different exponential decay processes, which are attributed to the percolation structure and isolated cluster structure.

The stretching and bending modes of water and the CF_2 combination mode represent the cluster and the polymer network, respectively. The CF_2 combination band intensity trace is consistent with the weight loss trace, giving comparable dual decay times, and its intensity increment is consistent with the dimensional change of the shrinking membranes. The shrinkage of the membrane is anisotropic, with contracting width and length but constant thickness. The water IR intensity loss traces also imply two distinct decay processes but show large deviation from the weight loss profile. The comparison between the relative water IR intensity

loss traces and the weight loss profile for LWLN clearly shows that using IR spectra as a quantitative measurement of water content is not warranted for Nafion. During dehydration, the intensity of the IR absorption of water in Nafion decreases significantly more than the extent of water loss. A model for this inconsistency has been presented on the basis of the dependence of the IR intensity of the water bands on the size of the aqueous clusters in the membrane structure.[5,22,23]

Acknowledgment. The authors gratefully acknowledge the assistance of The Lord Foundation of North Carolina, Bruker Optics, TA Instruments-Waters, LLC., and Duke University for support of this work and thank D. Bruce. Chase, E.I. Du Pont de Nemours & Co., for the donation of the Nafion membrane. Y.K. acknowledges FAPESP (99/10289-9) for a travel grant for work at Duke University.

References and Notes

(1) Sondheimer, S. J.; Bunce, N. J.; Fyfe, C. A. *J. Macromol. Sci., Rev. Macromol. Chem. Phys.* **1986**, *C26*, 351−413.
(2) Heitner-Wirguin, C. *J. Membr. Sci.* **1996**, *120*, 1−33.
(3) Gierke, T. D.; Hsu, W. Y. *Macromolecules* **1982**, *15*, 101−105.
(4) Bunker, C. E.; Rollins, H. W.; Ma, B. *J. Photochem. Photobiol., A* **1999**, *126*, 71−76.
(5) Gebel, G. *Polymer* **2000**, *41*, 5829−5838.
(6) Elliott, J. A.; Hanna, S.; Elliott, A. M. S.; Cooley, G. E. *Polymer* **2000**, *42*, 2251−2253.
(7) Gebel, G.; Lambard, J. *Macromolecules* **1997**, *30*, 7914−7920.
(8) Yeo, S. C.; Eisenberg, A. *J. Appl. Polym. Sci.* **1977**, *21*, 875−898.
(9) De Almeida, S. H.; Kawano, Y. *J. Therm. Anal. Calorim.* **1999**, *58*, 569−577.
(10) Deng, Q.; Wilkie, C. A.; Moore, R. B.; Mauritz, K. A. *Polymer* **1998**, *39*, 5961−5972.
(11) Feldheim, D. L.; Lawson, D. R.; Martin, C. R. *J. Polym. Sci., Part B: Polym. Phys.* **1993**, *31*, 953−957.
(12) Eisenberg, A.; Kim, J. S. *Introduction to Ionomers*; John Wiley & Sons: New York, 1998.
(13) Falk, M. *ACS Symp. Ser.* **1982**, *180*, 139−170.
(14) Sondheimer, S. J.; Bunce, N. J.; Lemke, M. E.; Fyfe, C. A. *Macromolecules* **1986**, *19*, 339−343.
(15) Gates, C. M.; Newman, J. *AIChE J.* **2000**, *46*, 2076−2085.
(16) Elliott, J. A.; Hanna, S.; Elliott, A. M. S.; Cooley, G. E. *Macromolecules* **2000**, *33*, 4161−4171.
(17) Laporta, M.; Pegoraro, M.; Zanderighi, L. *Phys. Chem. Chem. Phys.* **1999**, *1*, 4619−4628.
(18) Xie, G.; Okada, T. *Z. Phys. Chem. (Munich)* **1998**, *205*, 113−125.
(19) Buzzoni, R.; Bordiga, S.; Ricchiardi, G.; Spoto, G.; Zecchina, A. *J. Phys. Chem.* **1995**, *99*, 11937−11951.
(20) Falk, M. *Can. J. Chem.* **1980**, *58*, 1495−1501.
(21) Ludvigsson, M.; Lindgren, J.; Tegenfeldt, J. *Electrochim. Acta* **2000**, *45*, 2267−2271.
(22) Devlin, J. P.; Sadlej, J.; Buch, V. *J. Phys. Chem. A* **2001**, *105*, 974−983.
(23) Devlin, J. P.; Joyce, C.; Buch, V. *J. Phys. Chem. A* **2000**, *104*, 1974−1977.
(24) Wang, Y.; Kawano, Y.; Aubuchon, S. R.; Palmer, R. A. Manuscript in preparation.
(25) Samms, S. R.; Wasmus, S.; Savinell, R. F. *J. Electrochem. Soc.* **1996**, *143*, 1498−1504.
(26) Nemat-Nasser, S.; Li, J. Y. *Appl. Phys.* **2000**, *87*, 3321−3331.
(27) Dreyfus, B.; Gebel, G.; Aldebert, P. *J. Phys. (Paris)* **1990**, *51*, 1341−1354.
(28) Freger, V.; Korin, E.; Wisniak, J. *J. Membr. Sci.* **1999**, *160*, 213−224.
(29) Buck, U.; Huisken, F. *Chem. Rev.* **2000**, *100*, 3863−3890.
(30) Sadlej, J.; Buch, V.; Kazimirski, J. K.; Buck, U. *J. Phys. Chem. A* **1999**, *103*, 4933−4937.

MA020156E